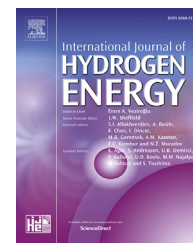


Available online at www.sciencedirect.com

ScienceDirect

journal homepage: www.elsevier.com/locate/hydro

Biogas steam reformer for hydrogen production: Evaluation of the reformer prototype and catalysts

Celso Eduardo Tuna ^{a,*}, José Luz Silveira ^a, Márcio Evaristo da Silva ^a,
Ronney Mancebo Boloy ^b, Lúcia Bolini Braga ^a, Nestor Proenza Pérez ^b

^a São Paulo State University, Faculty of Engineering at Guaratinguetá, Department of Energy, Laboratory of Optimization of Energy Systems (LOSE), Brazil

^b Federal Center of Technological Education Celso Suckow da Fonseca (CEFET/RJ), Angra dos Reis Campus, Brazil

ARTICLE INFO

Article history:

Received 12 September 2017

Received in revised form

10 November 2017

Accepted 3 December 2017

Available online 29 December 2017

Keywords:

Hydrogen production

Biogas steam reforming

Steam reformer

Catalysts

ABSTRACT

This work aims to investigate a biogas steam reforming prototype performance for hydrogen production by mass spectrometry and gas chromatography analyses of catalysts and products of the reform. It was found that 7.4% Ni/NiAl₂O₄/γ-Al₂O₃ with aluminate layer and 3.1% Ru/γ-Al₂O₃ were effective as catalysts, given that they showed high CH₄ conversion, CO and H₂ selectivity, resistance to carbon deposition, and low activity loss. The effect of CH₄:CO₂ ratio revealed that both catalysts have the same behavior. An increase in CO₂ concentration resulted in a decrease in H₂/CO ratio from 2.9 to 2.4 for the Ni catalyst at 850 °C, and from 3 to 2.4 for the Ru catalyst at 700 °C. In conclusion, optimal performance has been achieved in a CH₄:CO₂ ratio of 1.5:1. H₂ yield was 60% for both catalysts at their respective operating temperature. Prototype dimensions and catalysts preparation and characterization are also presented.

© 2017 Hydrogen Energy Publications LLC. Published by Elsevier Ltd. All rights reserved.

Introduction

Global warming is caused mainly by an excessive fossil fuel use, which has encouraged researchers to develop studies on efficient technologies and renewable sources for generating clean energy in order to replace traditional sources being used nowadays. Hydrogen is a relevant alternative for reducing environmental impacts which are usually caused by greenhouse gas emissions from fossil fuel use, since it is produced sustainably from renewable energy sources [1]. The most representative example of fuel to produce hydrogen is biogas that is typically generated by anaerobic digestion or biomass fermentation [2]. The main components of biogas are methane (CH₄) 50–70 vol % and carbon dioxide (CO₂) 25–50 vol

%, which also contains <1 vol% H₂ and <3 vol% H₂S, as well as traces of NH₃ [3]. Catalytic steam reforming is the most common process to obtain hydrogen, which is usually chosen due to its high efficiency. Moreover, its simplicity and low implementation costs should be compared to other technologies, such as partial oxidation reforming, auto-thermal reforming, dry reforming, and dry oxidation reforming [4]. This technology has been widely applied in chemical industries for large scale H₂ production, which is accountable for 50% of hydrogen generated worldwide by using natural gas as main hydrocarbon source [5]. It is a well-known process which has been described by several authors, e.g. Steinberg [6] and Poirier [7] who reported hydrocarbon reactions, like those of methane, naphtha and ethanol with water (pre-vaporized by a steam

* Corresponding author.

E-mail addresses: celso.tuna@feg.unesp.br (C.E. Tuna), juseluz@feg.unesp.br (J.L. Silveira), evaristom@yahoo.com.br (M.E. da Silva), ronney.boloy@cefe-rj.br (R.M. Boloy), luciabraga@gmail.com (L.B. Braga), nestor.perez@cefet-rj.br (N.P. Pérez).
<https://doi.org/10.1016/j.ijhydene.2017.12.008>

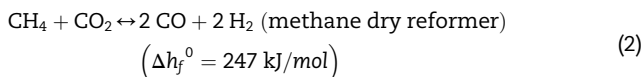
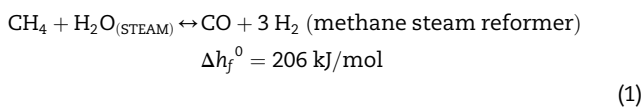
0360-3199/© 2017 Hydrogen Energy Publications LLC. Published by Elsevier Ltd. All rights reserved.

Nomenclature

Δh_f^0	Enthalpy of formation [kJ/kmol]
HTS	High Temperature Shift
LTS	Low Temperature Shift
MCFC	Molten Carbonate Fuel Cell
RWGS	Reverse Water Gas Shift
SOFC	Solid Oxide Fuel Cell
SRB	Steam reform of Biogas
TCD	Thermal conductivity detector
TPO	Temperature programmed oxidation
TPR	Temperature programmed reduction
WGS	Water Gas Shift

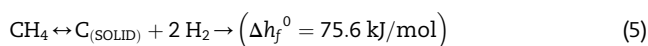
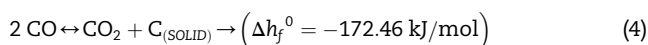
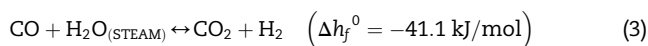
generator). The reactions that occur in this process primarily produce H_2 , CO_2 , CO and CH_4 , but there is no set quantity for these compounds whose concentration depend on several factors, such as reagents concentration, temperature and pressure of the reformer, as well as the physical and chemical characteristics of the chosen catalyst.

Steam reform of biogas (SRB), according to Bollini et al. [1], consists essentially in methane steam reforming and methane dry reforming as the following reactions:



Reaction (1) is the overall reaction that occurs in the steam reforming process and occurs at temperatures between 650 and 850 °C, thus obtaining H_2 yields of 60–70%, and the H_2/CO ratio is generally three, i.e. the most appropriate ratio for H_2 production [4]. **Reaction (2)** depicts methane dry reforming, which generally occurs at temperatures ranging between 700 and 900 °C by using a CH_4/CO_2 molar ratio of 1–1.5, with H_2 yields of around 50%. This reaction is more suitable for Fischer-Tropsch synthesis of biogas to produce liquid hydrocarbons and oxygenated derivatives, thus yielding H_2/CO ratio close to 1. Both reactions are highly endothermic and are favored by low pressures and high temperatures.

In addition to these main reforming reactions, other reactions can occur simultaneously that modify the equilibrium conversion of CO_2 and CH_4 , which are going to be presented as follows [4]:



Reaction (3) corresponds to the Water-Gas Shift Reaction (WGS), whose catalysts and reaction temperatures can be found in **Table 1**. The process can operate at high (HTS) or low (LTS) temperatures for eliminating CO produced in the

Table 1 – Catalysts and temperatures in the shift reactor [8].

Catalyst based on Cu/Fe/Cr →	Reactions HTS (250–450 °C)
Catalyst based on Cu/Zn →	Reactions LTS (150–250 °C)

reforming reactor, which enables the production of an additional amount of H_2 [4]. Unlike other reactions, it is exothermic and may occur at lower temperatures.

Boudouard's reaction (Eq. (4)) describes carbon formation by carbon monoxide decomposition. This reaction is very important for the process, since it is responsible for solid carbon deposition in catalysts. Methane dehydrogenation, shown in reaction (Eq. (5)), is one of the reactions that produce hydrogen while the reforming process is taking place, which also occurs in the reformer.

In biogas steam reforming processes, numerous supported catalysts have been tested. Catalysts are substances that are used in chemical reactions with the aim of accelerating them without being depleted. The materials which are mostly used as catalysts are palladium, ruthenium, iridium, tungsten, manganese, iron, silver, tantalum, titanium, vanadium, nickel, copper, and platinum [9]. In **Table 2**, examples of commonly used catalysts and their operating temperatures are listed, as well as the preparation technique being used. In the reforming process, most catalytic components are Ni-based, as Ni/Al_2O_3 [10]. This fact is due to the low cost of the component and its satisfactory efficiency.

Many supported catalysts in steam reforming have been tested, specially Ni-based catalysts, by some researchers, such as Kolbitsch et al. [12], Goula et al. [17], Urasaki et al. [18], Fonseca et al. [19] and Sabirova et al. [20]. However, one of the main problems of Ni-based catalysts is that they are subject to several types of deactivations, e.g. sintering, oxidation, carbon deposition and sulfur poisoning [15]. Among them, the most serious one is the formation of carbon deposits on catalysts which, consequently, lead to a blockage of catalyst pores by the deposited carbon, a separation of the catalyst by its support and lock on gas flow, due to an increase in pressure caused by pore blockage [21]. It occurs when the decomposition reaction of carbon monoxide, together with the decomposition reaction of methane (**Reaction 5**) are faster than the carbon removal rate is [4].

One common way to avoid these problems is to add suitable promoters that increase the stability of Ni-based catalysts, or to introduce a second metal component to form a

Table 2 – Catalysts for the biogas steam reforming system.

Catalyst	Preparation technique	Temp. (°C)
15% Ni/10% ZrO_2/Al_2O_3 [3]	Co-impregnation	500–700
5% Ni/5% La_2O_3/Al_2O_3 [11]	Impregnation/Calcination	550–800
11,5% Ni/ Al_2O_3 [8]	Reduction	650–850
CaO/Al_2O_3 [12]	Impregnation	650–860
5% Pt/ $\gamma-Al_2O_3$ [13]	Impregnation	500–900
Ni/Mg/ Al_2O_4 [14]	Impregnation	650–800
Ni_3Al [15]	Impregnation	600–800
Ni–Ti xerogel [16]	Sol-gel/Calcination	200–700

bimetallic catalyst system so as to inhibit carbon formation [22]. Some studies have used these techniques, some of which were reported by Xu et al. [22] by using Ni–Co/La₂O₃–Al₂O₃ catalysts. Therdthianwong et al. [3] and Angeli et al. [23] report the use of ZrO₂ as Ni/γ-Al₂O₃ promoter. The use of other oxides, such as K, Sn, Mn and Ca, has been reported by Luna and Iriarte [24]. The use of noble metals, such as Rh, Ru, Pt, and Pd, has also been studied by many researchers [25–29].

However, it is evident that these types of bimetallic or pure catalysts are of difficult commercialization due to their complex transportation and elevated costs. Thus, intensive research efforts are currently being made in order to improve the performance and lifetime of alumina-supported nickel catalysts [30].

Thereby, the principal aim of the present work is to investigate the performance of NiAl₂O₄/γ-Al₂O₃ catalyst in order to compare its catalytic activity under CH₄/CO₂ reforming conditions and evaluate its resistance to carbon formation with a Ru/γ-Al₂O₃ catalyst. The effect of operating conditions (CH₄/CO₂ molar feed gas ratio of 1.5:1 and 1:1) and temperature (650–850 °C) on CH₄, CO₂ conversions and H₂/CO ratio for the two catalysts under study by employing an experimental pilot unit.

Experimental procedure

Catalyst preparation

Aluminum oxide (γ-Al₂O₃) was used as supporting material for Ni and Ru based catalysts. The support γ-Al₂O₃ was prepared by a precipitation process with solutions of aluminum nitrate Al(NO₃)₃·9H₂O; (0.5 mol/l) and ammonium hydroxide NH₄OH (6 mol/l). The process consists in adding an aluminum nitrate solution by using a peristaltic pump with constant flow into the ammonium hydroxide solution under constant stirring and maintaining pH ≥ 10. After precipitation, the system was left at rest for aging during 16 h at 298 K, and then it was filtered and washed with distilled water at 333 K to remove the precipitating agent until it presented neutral pH. The obtained aluminum hydroxide was dried in a vacuum oven during 16 h at a temperature of 343 K. After the material was cooled in a desiccator, it was crushed and then burned in a muffle furnace at 773 K during 3 h at a heating rate of 10 °C/min.

Conventional incipient wetness impregnation was used to prepare the Ni/γ-Al₂O₃ and Ru/γ-Al₂O₃ catalysts. The impregnation solutions were prepared by dissolving nickel nitrate hexahydrate Ni(NO₃)₂·6H₂O and Ruthenium chloride trihydrate RuCl₃·3H₂O with the required concentration values in order to obtain final catalysts with Nickel content of 7.5% and Ruthenium content of 3.4%, respectively, which were then impregnated onto an Al₂O₃ support. It was employed distilled water as liquid in an automatic pipette of 10 ml. After impregnation, the catalysts were dried in a vacuum oven for 16 h at 343 K. Then, they were calcined at temperatures from 300 K to 773 K at 10 °C/min heating rate and the same temperature was kept for 1 h. Ni/γ-Al₂O₃ was calcined again in air at 850 °C for 10 h in order to enhance NiO/Al₂O₃ interaction to form NiAl₂O₄. Finally, the catalysts were crushed and sieved into granules with particle sizes ranging between 0.3 and

0.5 mm before being loaded onto the reactor for experimental testing.

Catalyst characterization

Temperature Programmed Reduction (TPR) experiments were carried out in a quartz fixed bed reactor by using a CHEMBET 3000 analyzer. 0.15 g of calcined catalysts was heated from 27 °C to 200 °C at a heating rate of 10 °C/min and flow rate of 50 ml/min for 1 h. After being dried, the material was cooled to 110 °C. Once a certain temperature is reached, a reduction mixture was formed by 5% H₂/N₂ at the same flow rate (50 ml/min) to replace the carrier gas. After stabilization, the temperature was raised to 1000 °C at a rate of 10 °C/min. H₂ consumption during TPR was monitored continuously by a thermal conductivity detector (TCD).

To determine the amount of carbon deposited on the catalysts, they were submitted to Temperature Programmed Oxidation (TPO) and Temperature Programmed Reduction (TPR) in the presence of methane and oxygen, respectively, which were then subjected to thermogravimetric and mass spectrometry analyses. These analyses aim to determine reduction and oxidation temperatures of materials that were identified by changes in mass and resulting gases. About 50 mg of catalysts was placed in a crucible under gaseous mixture flow comprising 10% CH₄ and 10% CO₂ with argon as being the carrier gas (Ar). In the case of TPR, a total flow of 80 ml/min is kept. For TPO, it was used 20% of O₂. In both cases, 2% of He was used as reference for calculating the concentration of gases it had produced. The materials were subjected to heating from 25 to 1000 °C at a rate of 5 °C/min.

Catalyst activity experiments

The catalysts that had already been analyzed in the previous section were evaluated in an experimental pilot unit (Fig. 1) which was designed and built in the Laboratory of Optimization of Energy Systems (LOSE). The cycle comprises a tank for distilled water (1), a metering pump (2), a vaporizer (3), a biogas injection system (4), a biogas/steam mixing chamber (5), a reformer (6), a cooling system (7), a water-gas shift reactor (8), a cooling system (9), a buffer tank with a manometer for checking the synthesis gas pressure (10), an electronic purificator (11), a coalescing filter (12), outlet for the condensate (13) and another for the synthesis gas (14).

The catalyst was evaluated at atmospheric pressure in a fixed-bed reactor (Reformer and water-gas shift reactor) which was connected after the biogas/steam mixing chamber was placed, whose dimensions can be seen in Fig. 2. The biogas/steam mixture enters into the reformer at the bottom of the reactor through 0.003 m holes distributed along the support plate of the reactor, which is 0.01 m thick. Thermal insulation was performed with a refractory and ceramic fiber. With the purpose of achieving better temperature control and contact time between the catalyst and the achievable mixture, the reformer must have the following characteristics: 0.114 m of diameter between the isolation wall and the reformer external wall and 0.0762 m of internal bed and a bottom-perforated plate with 0.003 m holes, totaling approximately 30% of free area. It was installed a thermocouple for

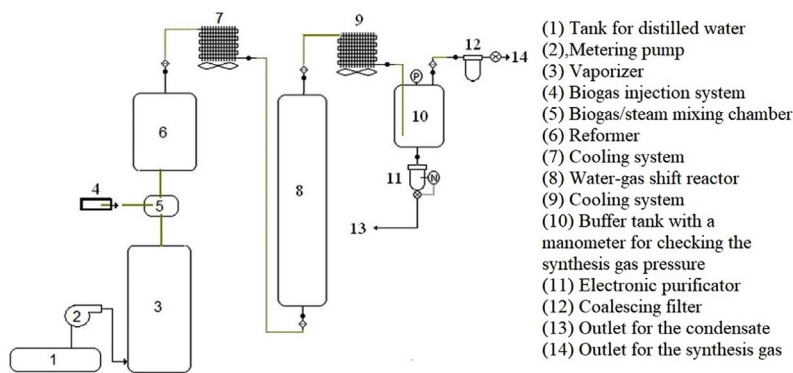


Fig. 1 – Schematic and prototype of the biogas steam reforming system.

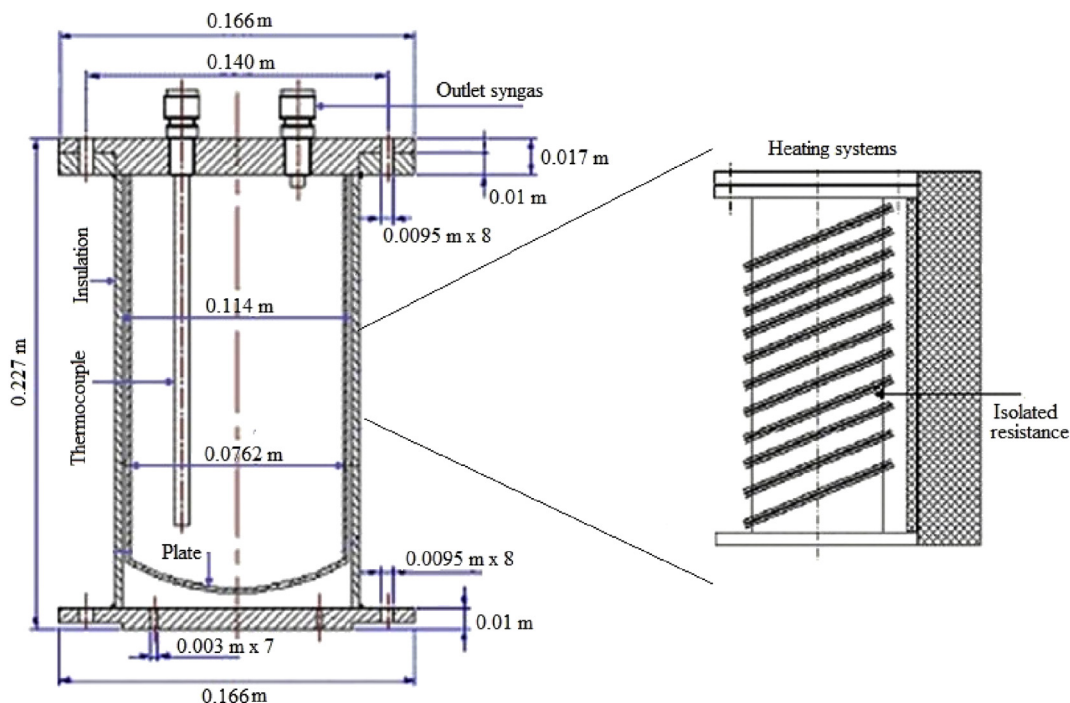


Fig. 2 – Reformer schematic.

temperature control and an outlet for the syngas to be released from reforming reactions. A schematic comprising the heating system, thermal insulation composed of refractory products and isolated resistance with beads can be seen in Fig. 2.

The shift reactor, presented in Fig. 3, consists of a thermally insulated cylinder, with a built-in bed and a perforated plate to provide support for the catalytic converters to interact with the synthesis gas from the reforming reactor. The synthesis gas of the reformer, after the cooling system, enters into the shift reactor at the bottom of the reactor through a connecting tube with 0.004 m diameter inserted in the support plate which is 0.01 m thick. The internal diameter is similar to that of the reformer to promote the conversion of part of the CO into CO₂ and the production of additional H₂. The cooling system of the produced synthesis gas, which was installed after the reform and Shift reactions can be also seen in Fig. 3,

which is composed of a cooling system through conduction and convection (9), a buffer tank with a manometer to check the pressure of the synthesis gas (10), an electronic purificator (maximum pressure of 175 psi) for condensate removal (11), coalescent filter to remove the remaining moisture in the synthesis gas (12) and two outputs, (13) and (14), respectively, the condensate output and the synthesis gas output with low moisture content.

In the reform, it was used a total flow rate of 2.5 l/min which is controlled by mass flow meters, being 20% biogas mixture and balance in Ar with 1% He. The fixed bed reactor was loaded with 1200 g of catalyst, and heated up to reduction temperature, corresponding to each type of catalyst (heating rate of 10 °C/min). Two compositions were used for biogas, the first one containing 60% CH₄ and 40% CO₂, which means a molar fraction ratio of CH₄:CO₂ = 1.5:1 and the second one with 50% CH₄ and 50% CO₂ (CH₄:CO₂ = 1:1). For the steam concentration, it was used a constant value of one and a half times greater

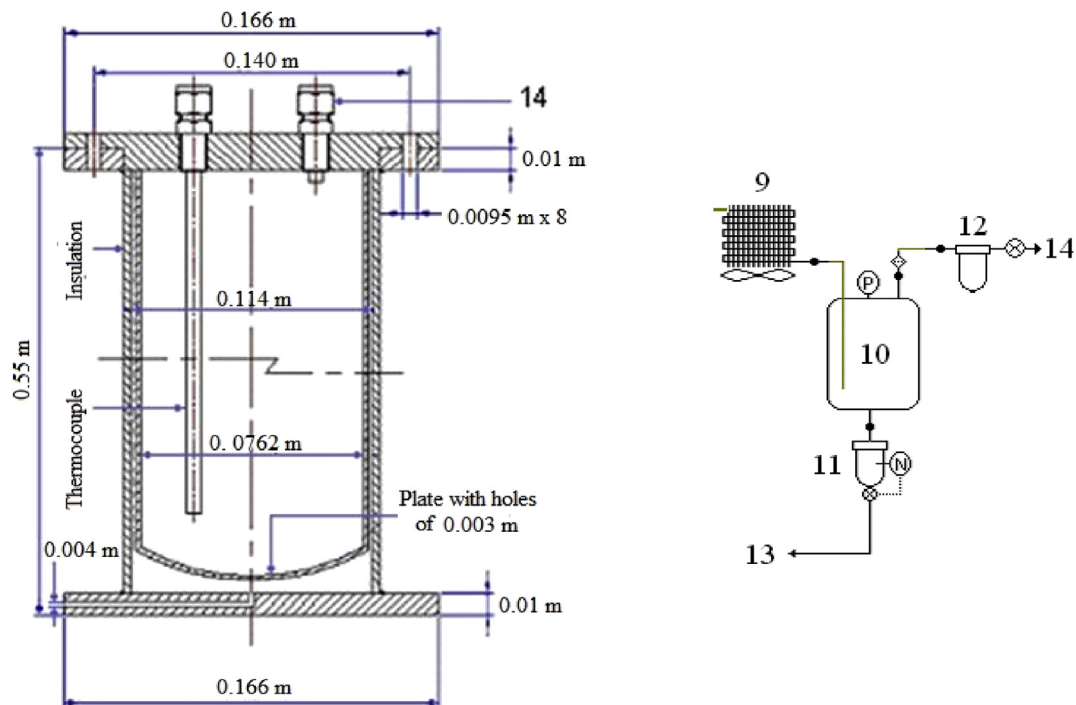


Fig. 3 – Schematic drawing of the Shift reformer and cooling system.

than the concentration of biogas (Steam/Biogas = 1.5). The biogas mixture was composed of 20% of the compound itself ($\text{CH}_4:\text{CO}_2 = 1.5:1$ or $1:1$), 79% argon and 1% helium, which is necessary for calculating the concentration of gases. The tests lasted thirty minutes for each catalyst, or until a considerable deactivation of the catalyst was identified. Once tested, the catalysts were reactivated by using O_2 flow, in order for the material to be reoxidized and the carbon deposits to be removed. Reforming biogas tests were performed at different temperatures (650–850 °C). The concentrations of gaseous products H_2 , CO_2 , N_2 , CH_4 and CO in the product gas were analyzed by mass spectrometry and gas chromatography.

Results and discussion

Characterization of catalysts by the TPR and TPO tests

$\text{NiAl}_2\text{O}_4/\gamma\text{-Al}_2\text{O}_3$ catalyst

Fig. 4 shows the temperature programmed reduction curve for the fresh Ni-base catalyst. The TPR curve analysis suggests that the reduction of bulk nickel oxide or NiO species, either with or without a weak interaction with the Al_2O_3 support, was negligible. It indicates that if these species were present in the catalyst, they would be in a very small quantity because this process occurs at relatively low temperatures (lower than 550 °C) [31] and no peak was observed in that range. The first peak was observed at a temperature of 558 °C and it can be attributed to a small quantity reduction of non-stoichiometric nickel aluminate species (NiAl_xO_y) present in the surface, which is consistent with previous reports [17,32]. The major peak presented a narrow shaped peak at 780 °C, which can be assigned to the presence of the NiAl_2O_4 phase [22] being

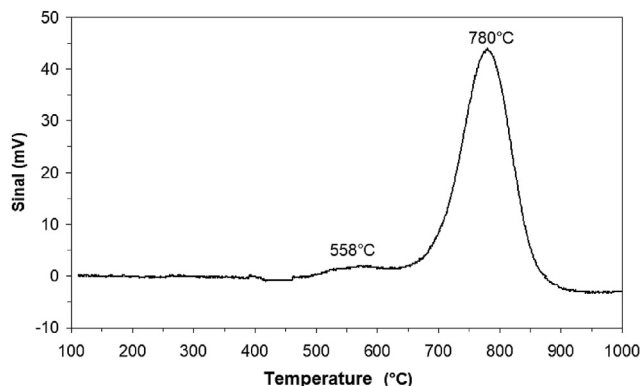


Fig. 4 – Ni catalyst (TPR) with 5% H_2/N_2 , 10 °C/min and 50 ml/min.

formed by the diffusion of nickel ions in the support. These peaks confirm the existence of an interfacial NiAl_2O_4 layer on the catalyst that could interrupt the growth of Ni metallic particles, thus stabilizing the formation of small size Ni metallic crystallites under reduction conditions. This exerts a favorable effect on performance, stability and lifetime of the catalyst in the biogas steam reforming reaction, given that nickel aluminate interacts more strongly with nickel metallic and alumina in comparison with their interaction [33].

Catalyst reducibility has been studied by several researchers. Zielinski [34] investigated the influence of different wt% of Ni (2–20%) on a $\text{Ni}/\text{Al}_2\text{O}_3$ catalyst obtained by the impregnation method followed by calcination at 400 °C. For all samples, all reduction peaks were observed at a range of 400–500 °C, which was attributed to NiAl_2O_4 . In another study reported by Zhang et al. [35], the alumina support was

calcined at 600 °C after impregnation with nickel. For a sample with 2 wt% Ni, only one peak at 527 °C was observed, which was assigned to the reduction of nickel aluminates surface. Three significant reduction peaks were detected in Salhi et al. [30] and Zhou et al. [36] studies. In these cases, the reported TPR that corresponds to the reduction of NiAl_2O_4 were 800 °C and 830 °C, respectively. These results are different from the one reported in this study, probably in the first two cases, by the differences in calcination temperature being used in these works. As regards the study of Salhi et al. [30], the difference can be influenced by the catalyst preparation method, where the sol-gel and incipient wetness impregnation methods were used in each case. Finally, the used bimetallic catalyst $\text{Ni}/\gamma\text{-Al}_2\text{O}_3$ /alloy in the study reported by Zhou et al. [36] may be the cause of such differences.

Fig. 5 shows the TPR in the presence of 10% CH_4 and 10% CO_2 , respectively, followed by thermogravimetric and mass spectrometry analyses. It is observed a small mass loss occurring from 653 °C, which is probably due to a small percentage of existing aluminate species in the catalyst, but the most significant weight loss occurred at 750 °C due to a complete reduction of NiAl_2O_4 coinciding with the H_2 -TPR test. It demonstrates that the most significant production of CO and H_2 (characteristic of the dry reforming) occurs from 800 °C. This result allows affirming that higher or equal temperatures are required than those of the steam reforming reactions in a fixed bed reactor. At 871 °C, there was an increase in mass, which is a characteristic phenomenon of carbon deposit. By considering mass reduction, it can be estimated that the material contains approximately 7.4% Ni, thus finally confirming the catalyst composition as being 7.4% $\text{Ni}/\text{NiAl}_2\text{O}_4/\gamma\text{-Al}_2\text{O}_3$. The catalyst appeared selective for the production of CO and H_2 , however, due to a reduced amount of the material used in the thermobalance tests, these results must be confirmed by the reforming tests in the pilot experimental installation.

The Temperature Programmed Oxidation (TPO) test (not shown here) showed an increase in catalyst mass due to its reoxidation. Moreover, the production of CO or CO_2 , due to the reaction of oxygen with the deposited carbon, has not been possible to be registered by mass spectrometry. Therefore, the absence of O_2 consumption signal in the deactivated catalyst

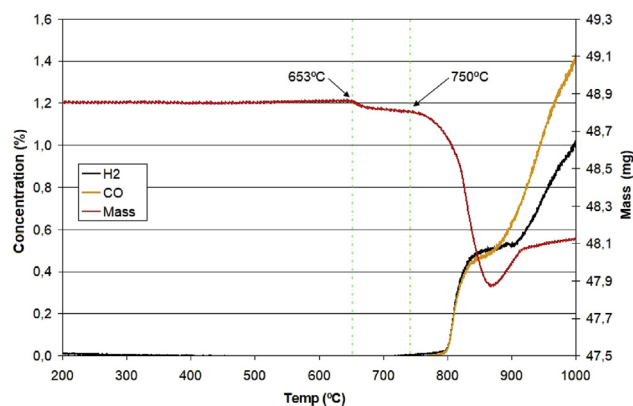


Fig. 5 – Ni catalyst (TPR) with 10% CH_4 and 10% CO_2 , 5 °C/min, and 80 ml/min.

is an indicator of low concentration of deposited carbon, thence indicating that there may be serious problems of carbon coking during the steam reforming test.

Ru/ $\gamma\text{-Al}_2\text{O}_3$ catalyst

The TPR profiles with 5% H_2/N_2 of Ru/ $\gamma\text{-Al}_2\text{O}_3$ catalyst are shown in Fig. 6. The identification of different species of ruthenium oxides, shown in Fig. 6a and b, is extremely difficult, since this metal evolves the RuCl_3 into different sub-oxides and, during TPR, other unknown species of ruthenium may be formed on the support surface [37]. TPR curves of Ru/ $\gamma\text{-Al}_2\text{O}_3$ catalyst shows a higher peak at 198 °C, which it is attributed to RuO_2 reduction in accordance with the results reported in literature. Koopman et al. [38] attributed a peak between 177 and 205 °C to the reduction of RuO_2 on silica, while Mazziari et al. [39] found a maximum peak at 197 °C and a low one at about 156 °C, which are attributed to the reduction of ruthenium oxide and ruthenium oxychloride, respectively. The different behavior of TPR profile shown in this study in comparison with others [38–40], (where only one or two peaks were observed), can be attributed to the catalyst preparation methods, as well as the calcination and reduction process used in each case [3,17,31,41].

Between 300 and 700 °C, the analysis of Fig. 6 makes it clear that the reductions are more intense in the pre-reduced material at 400 °C. This treatment favors the release of chlorine as ruthenium chloride, which is a very stable species that hinders the reduction Ru to state zero. However, RTP evidences a lower temperature reduction with the Ru catalyst if compared to that of Ni catalyst, which shows that it can favor the reaction with biogas since the element assumes metallic characteristics under less severe reaction conditions (lower temperature).

Fig. 7 shows the reducibility of Ru in the presence of 10% CH_4 and 10% CO_2 , respectively, followed by thermogravimetric and mass spectrometry analyses. A significant and rapid loss of mass occurred the moment a temperature of 470 °C was reached, due to a reduction of ruthenium oxide, whose results are consistent with those obtained during the reduction with H_2 . It is noticed that the production of CO and H_2 (characteristic of the dry reforming) occurs at 470 °C, which is a very low value obtained with the Ni catalyst (750 °C). Then, with this catalyst, it must be working at or above temperatures of 470 °C for steam reforming reactions occurring in a fixed bed reactor. By considering mass reduction, it can be estimated that the material contains approximately 3.1% Ru, thus finally confirming the catalyst composition as being 3.1% Ru/ $\gamma\text{-Al}_2\text{O}_3$. Moreover, it was verified an increase in mass at 900 °C, a characteristic phenomenon of carbon deposition formation.

The results of the Temperature Programmed Oxidation (TPO) after and before the TPR are shown in Fig. 8. Before the TPR, the material was not fully oxidized, where there was a mass increase from 150 °C to 300 °C, approximately, and a further increase after 635 °C. After the TPR, the TPO showed a loss of mass from 150 °C to 530 °C, which is characteristic of the oxidation of carbon deposits, but the production of CO or CO_2 was not observed by mass spectrometry, probably due to the low deposit concentration on the catalyst surface. The increase in mass registered after 530 °C is due to the catalyst reoxidation.

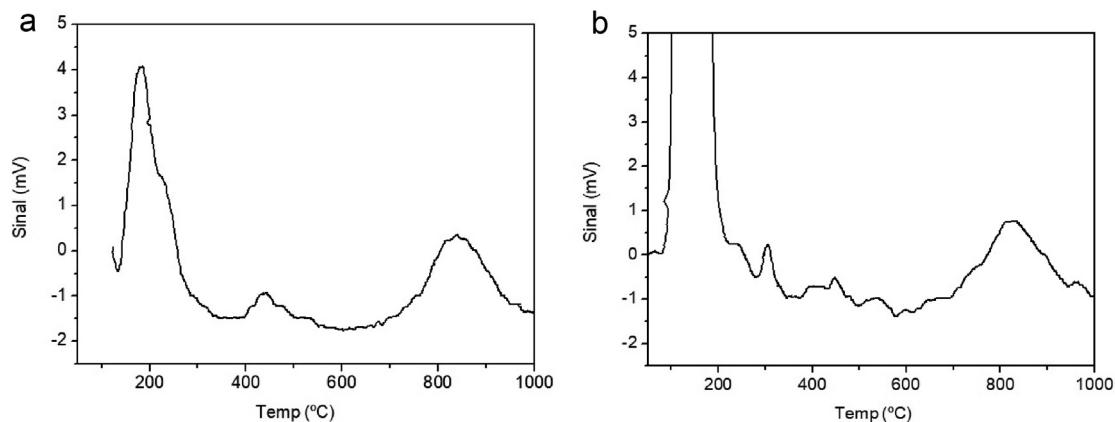


Fig. 6 – Ru catalyst (TPR) with 5% H₂/N₂. a) Material after impregnation and drying at 120 °C. b) Impregnated material, dried at 120 °C, and subjected to reduction with hydrogen at 400 °C.

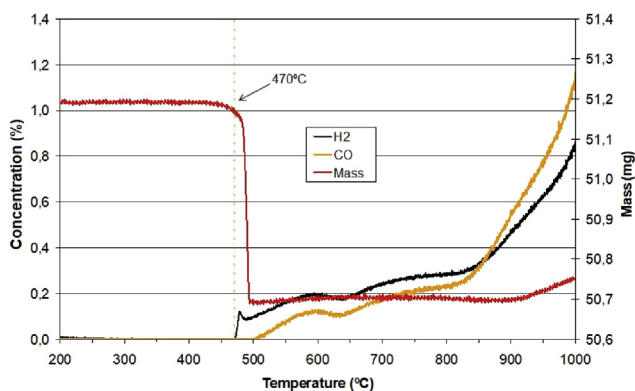


Fig. 7 – Ru catalyst (TPR) with 10% CH₄ and 10% CO₂.

Catalytic test on biogas steam reforming reaction

Reforming test with 7.4% Ni/NiAl₂O₄/γ-Al₂O₃ catalyst

The reforming tests for the Ni catalyst were performed at three temperatures: 750 °C, 800 °C, and 850 °C in an experimental steam reformer installation operating under atmospheric pressure. Two different compositions of biogas were investigated (CH₄:CO₂ = 1.5:1 and 1:1) with a constant steam/biogas feed ratio of 1.5 and gas hourly space velocity (GHSV) of

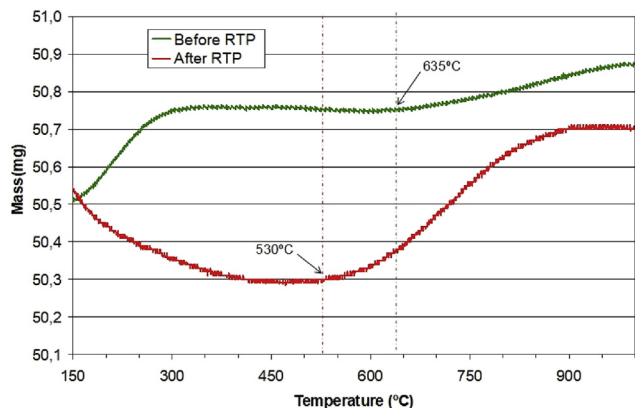


Fig. 8 – Mass curves during TPO of Ru catalyst with 20% O₂.

850 and 780 h⁻¹, respectively. All experiments lasted 30 min. The concentration curves were obtained from mass spectrometry and gas chromatography.

Fig. 9 shows the curves of the steam reforming of biogas (SRB) with a composition of CH₄:CO₂ = 1.5:1 with the nickel catalyst, in which temperatures of 750 °C, 800 °C, and 850 °C, respectively, were kept for 30 min. It was observed that, at temperatures ranging from 750 °C to 800 °C, there was no methane consumption, therefore the steam reforming reaction could not occur. However, when the material was analyzed at 850 °C, a small peak of unreacted CH₄ was found at the beginning of the experiment but, after a few minutes, the compound was completely consumed. During the experiment, it appears that the H₂/CO ratio obtains a value of 2.9, which is very close to the one proposed in literature as optimal for SRB (H₂/CO = 3) [4], thence evidencing high CH₄ conversion.

Thus, it is possible to conclude that the steam reforming reaction was preponderant over the dry reforming reaction (H₂/CO = 1), which can be verified by the presence of large amounts of steam along the reaction. This behavior is different than the one reported by Sahi et al. [30] who had used a NiO/γ-Al₂O₃ catalyst in which the increase of H₂ production was mainly due to the large production of coal on account of the CO₂ percentage being very low, therefore the WGS (water gas shift) reaction is not favored in such conditions. After 30 min of reform, the catalyst re-oxidation was accomplished, and it was found that there was no carbon deposition on the surface of the material, and that the release of CO₂ or CO had been below detectable value. It was observed oxygen consumption during 0.35 min, which is enough time for the catalyst reoxidation to occur. The average yield of H₂ and CO products of syngas were 60% and 21%, respectively, while CH₄ was thoroughly consumed.

Fig. 10 shows the gas production curves that were obtained during the steam reforming of the second composition of biogas (CH₄:CO₂ = 1:1), which was kept at 850 °C for 30 min, given that, in previous tests, the catalyst was not active at lower temperatures (750–800 °C). The results indicated a H₂/CO ratio of 2.3 during the reform. Note that methane was thoroughly consumed, i.e. an indicative of the reform

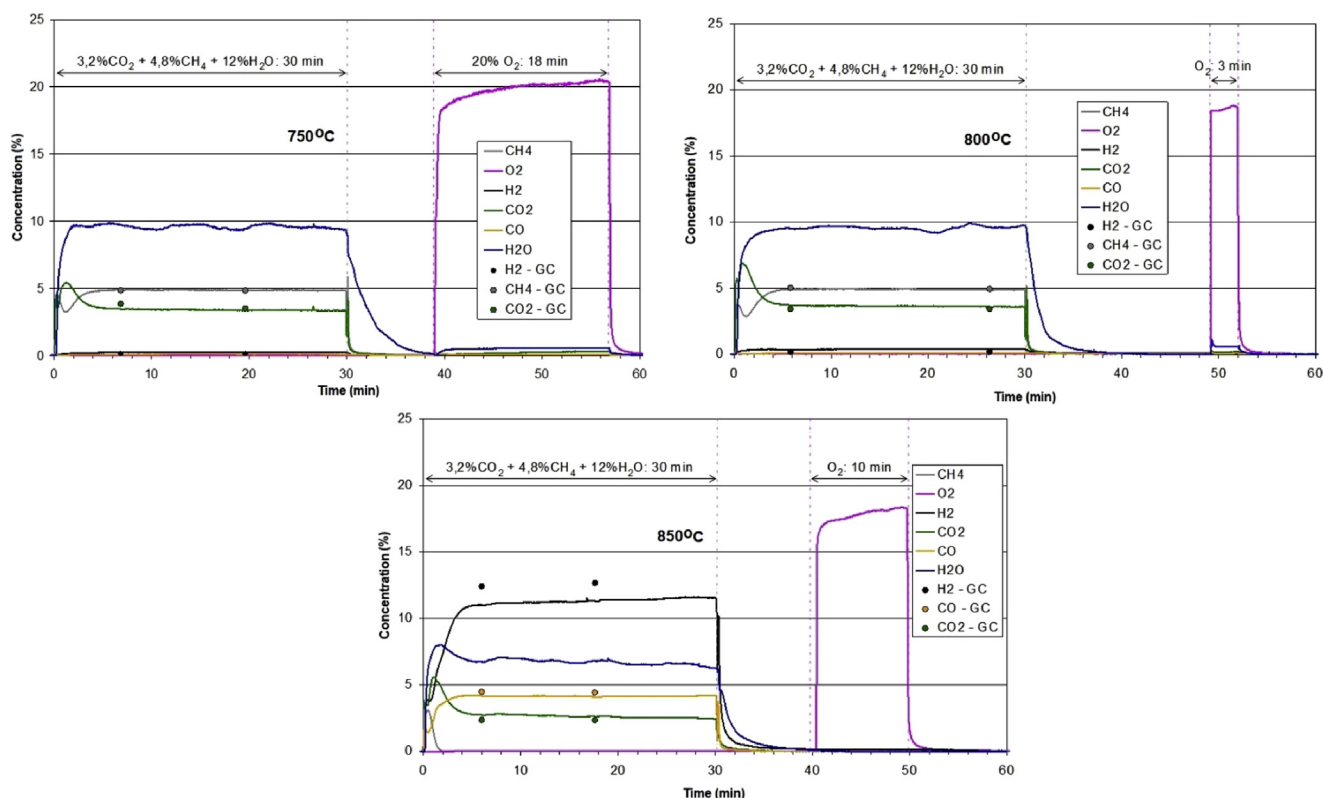


Fig. 9 – SRB with Ni catalyst ($\text{CH}_4:\text{CO}_2 = 1.5:1$; steam/biogas 1.5; pressure 1 bar; $\text{GHSV} = 850 \text{ h}^{-1}$).

occurrence. As the H_2/CO ratio is far from being ideal for a complete steam reforming occurrence, it can be affirmed that the biogas composition has a direct influence on whether the steam reforming process is predominant over the dry reforming process. It can be demonstrated by the CO_2/CO ratio being approximately equal to 1 and a larger concentration of CO_2 throughout the process (about 3.4%) if compared to the previous test (2.5%). As in the previous model ($\text{CH}_4:\text{CO}_2 = 1.5:1$), carbon deposition on the catalyst was not detected after catalyst re-oxidation.

From Figs. 9 and 10, a decrease in $\text{CH}_4:\text{CO}_2$ ratio afforded negligible effects on CH_4 conversion at the selected temperature (850°C). In contrast, H_2 yield and H_2/CO ratio decreased from 60% to 45% and 2.9 to 2.3, respectively, but CO_2 concentration in the synthesis gas increases while the CO remained almost constant. This behavior may be the result of a higher CO_2 concentration in the feed gas, which impairs the WGS reaction drive to decrease CO_2 conversion, as well as the increase in the competition between dry reforming and steam reforming processes [42]. Nevertheless, steam reforming takes

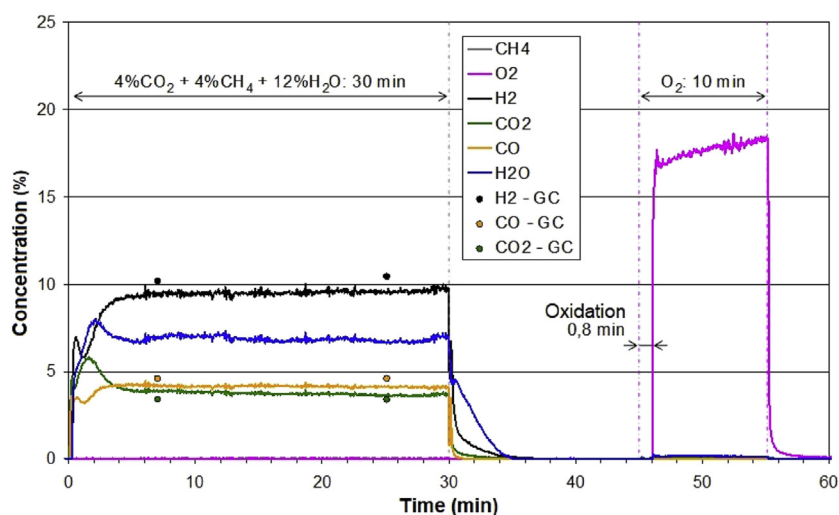


Fig. 10 – SRB with Ni catalyst ($\text{CH}_4:\text{CO}_2 = 1:1$; steam/biogas 1.5; pressure 1 bar; $\text{GHSV} = 780 \text{ h}^{-1}$).

place predominantly, since only 0.6% of CO_2 reacted with methane in the dry reforming reaction.

When relatively long-term stability tests (2 h, not shown here) were performed for a biogas composition of $\text{CH}_4:\text{CO}_2 = 1:1$, the H_2/CO ratio was 2.4 and methane was completely consumed. This small increase in H_2/CO ratio from the outset of the steam reforming process could be either linked to a catalytic dehydrogenation of CH_4 or the WGS reactions [43]. These two reactions produce hydrogen, but dehydrogenation also produces carbon that might have been gasified by steam during the reforming process, given the fact that there was no production of CO or CO_2 during the oxidation stage and no deactivation and coke deposition. Ni catalyst re-oxidation was performed in 1.8 min, i.e. enough time to restore maximum oxygen content. On the other hand, biogas in the ratio of $\text{CH}_4:\text{CO}_2 = 1.5:1.0$ behaved similarly in the long-term stability test in comparison with the one reported in Fig. 9.

Some studies about steam reforming processes using Ni catalysts have been reported, in which the steam reforming of biogas generally takes place over dry reforming processes [11,22,24]. However, there are few reports available in literature about the combination of both processes (steam and dry reforming process) [12]. Thus, its results from a combined use of steam reforming and dry reforming of methane are fundamental to find optimal operation process conditions, e.g. reactor temperature, in order to allow a viable process for producing synthesis gas from biogas without sintering or carbon deposition on the catalyst surface, which are the main problems faced in Ni/ $\gamma\text{-Al}_2\text{O}_3$ catalysts deactivation

[22]. The 7.4% Ni/ $\text{NiAl}_2\text{O}_4/\gamma\text{-Al}_2\text{O}_3$ catalyst, which was evaluated experimentally, has showed relevant catalytic performances: high CH_4 conversion, low carbon formation and H_2/CO ratio ≈ 3 . It can be assumed that Ni catalyst high performance and stability are mainly due to the formation of spinel NiAl_2O_4 , thus causing high dispersion of very small nickel particles (being able to form 6 nm Ni crystallites) [17]. Moreover, the active phase distribution (Ni^{2+}) along particular sites that were formed after the spinel reduction is consistent with previous works reported by other researchers [30,44,45].

On the other hand, its high resistance to coke deposition can be explained by the fact that the deposited carbon has a filamentous structure which allows the active metal to remain on the top of the carbon filament and, consequently, it remains accessible to reactants, thus resulting in a high and stable catalyst activity [24]. Another reason for such could be the high H_2/CO ratios (more than 2) which can alleviate the carbon deposition problem. It is widely accepted that if H_2/CO ratios are sufficiently high, the encapsulation of metal particles by the deposited carbon does not occur [45], therefore favoring catalytic activity. Presumably, this type of catalyst will be highly resistant to coking (over 100 h), which is based on a previous study developed by Ref. [36], thus it is expected high durability.

Reforming test with 3.1% Ru/ $\gamma\text{-Al}_2\text{O}_3$ catalyst

The tests for the reforming of biogas with $\text{CH}_4:\text{CO}_2 = 1.5:1$ with Ru catalyst were performed at temperatures of 650 °C, 700 °C and 750 °C.

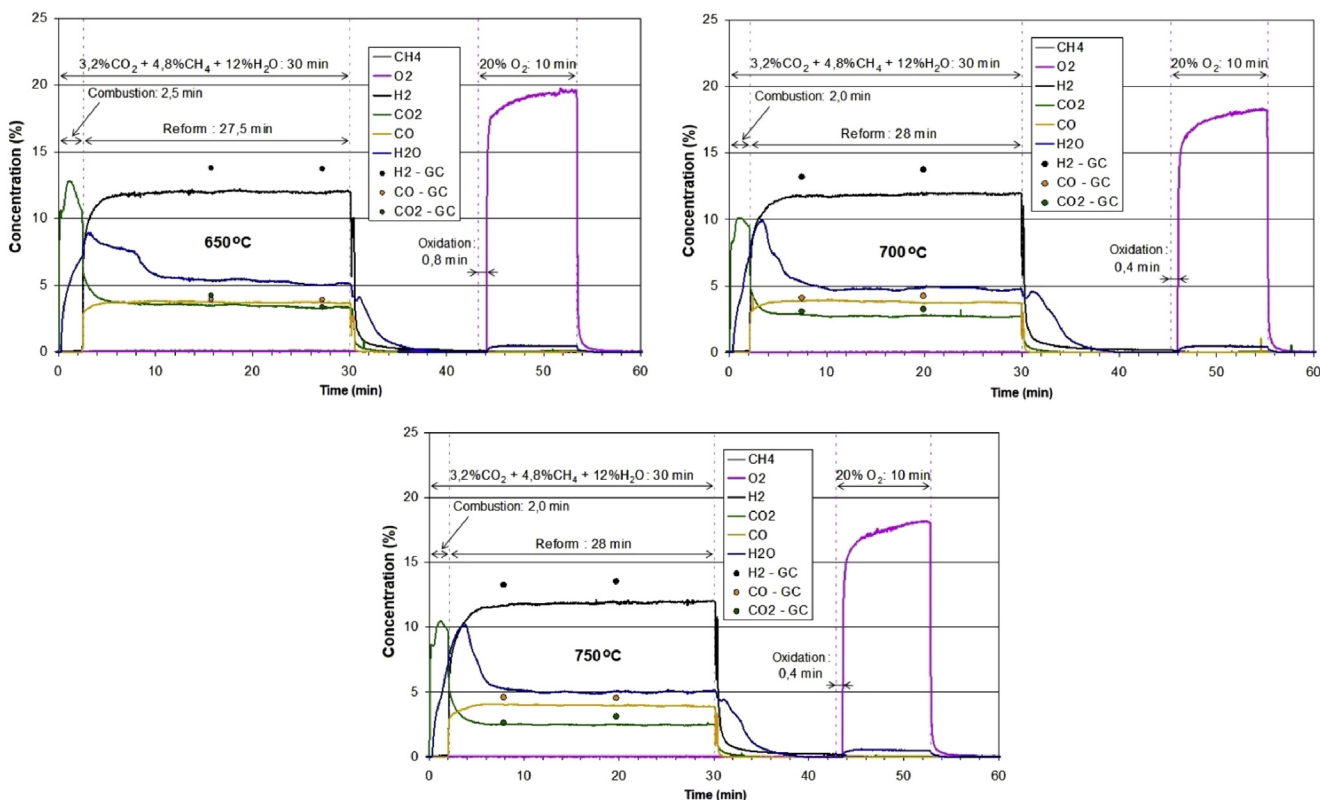


Fig. 11 – SRB with Ru catalyst ($\text{CH}_4:\text{CO}_2 = 1.5:1$; steam/biogas 1.5; pressure 1 bar; GHSV = 850 h^{-1}).

Fig. 11 shows the concentration curves of syngas produced for the steam reforming with the ruthenium catalyst kept during 30 min. It is possible to observe that an increase in temperature from 650 to 750 does not lead to a significant increase in H₂ or CO production, in accordance with [17], as it is well known that in order to increase the quantity of produced hydrogen, high temperatures are needed. For the reforming process carried out at 650 °C, the results were 2.5 min of combustion; 0.14% of unconsumed methane and an H₂/CO ratio of 3.5. This value indicates that the formation of H₂ occurred through the steam reforming preponderantly and by simultaneous reactions, like methane decomposition and WGS reaction. These two reactions produce hydrogen, while dehydrogenation produces carbon that might have been gasified by steam during the reforming reaction, given the fact that there was no CO₂ or CO production during oxidation. The concentration ratio of CO₂/CO was approximately 1, which allows assuming that the steam reforming, WGS and carbon gasification (disproportionation reaction) reactions occurred simultaneously at the same rate [17].

From Fig. 11, it is also possible to observe an increase in CO concentration and a decrease in H₂/CO ratio (~3.0) with increased temperature (700–750 °C), which is consistent with the fact that the WGS reaction is less favorable thermodynamically at higher temperatures [27,42]. These results suggested that as CO yield increases, H₂ remained almost constant, while CO₂ yield decreased at relatively high temperatures [46]. It can be explained by the increased contributions of dry reforming of methane and reverse water gas shift (RWGS) reaction to produce CO in the steam biogas reforming reaction [47], which implies that the CO₂ production rate via the WGS reaction is comparable to the dry reforming of CH₄ at 750 °C [42]. However, the steam reforming reaction is still predominant over the dry reforming reaction because the H₂/CO ratio was about 3.0, which is ideal for SRB [4]. Generally, CH₄ conversions increase as temperature does for all tested ranges, as found by Ref. [17]. The amount of unconsumed methane were 0.05% at 700 °C and 0.04% at 750 °C, respectively, i.e. much lower values than those reported at 650 °C.

The influence of CH₄:CO₂ ratio on inlet gas feed was also examined. Fig. 12 shows the catalyst behavior for a long-

term stability test (two hours) with CH₄:CO₂ ratio of 1:1 at 700 °C. When the inlet gas ratio decreases, it can be observed that H₂ yield decreased from 60% at an inlet gas ratio of 1.5:1–47.5% at a ratio of 1:1 by keeping the same catalyst temperature, which also leads to a decrease at a H₂/CO ratio of around 17%. These facts are consistent with previous studies reported by Refs. [27,48]. In contrast, CO₂ concentration increased significantly as the CH₄:CO₂ ratio decreased from 15% to 25%. This increase in CO₂ concentration brings about negligible effects on CH₄ conversion, thus maintaining the unconsumed methane at 0.04%. The aforementioned could be explained by a decrease in CO₂ conversion, thus indicating that a greater quantity of CO₂ is produced as a result of the combination of methane steam reforming and WGS reactions, which is greater than that consumed by the dry reforming and the RWGS reactions [48]. Furthermore, the results of the long-term stability test clearly indicate that, after two hours of reaction, both the conversion and selectivity tend to behave similarly, which is fairly stable along the reaction, in which deactivation or carbon deposition on the catalyst surface is not observed. It is expected high activity and good stability in the long-term for this type of catalyst, since these are the main advantages of catalysts based on noble metals, such as Ru, with high resistance to carbon deposition [48].

Comparison of nickel and ruthenium catalysts from the performance evaluation

It was performed an evaluation of two catalytic materials in the biogas steam reforming reaction. Catalysts containing about 7.4% of Ni (7.4% Ni/NiAl₂O₄/γ-Al₂O₃) and 3.1% of ruthenium (3.1% Ru/γ-Al₂O₃) supported on a gamma alumina were analyzed. The materials were characterized by the reduction reaction with hydrogen with a chemisorption equipment, followed by oxidation in a thermo balance attached to a mass spectrometer. In Table 3, the main comparative results are listed.

In comparison with the Ni/NiAl₂O₄/γ-Al₂O₃ catalyst, the analysis showed a lower temperature reduction for ruthenium. At this point, Ru/γ-Al₂O₃ has an advantage, since CO

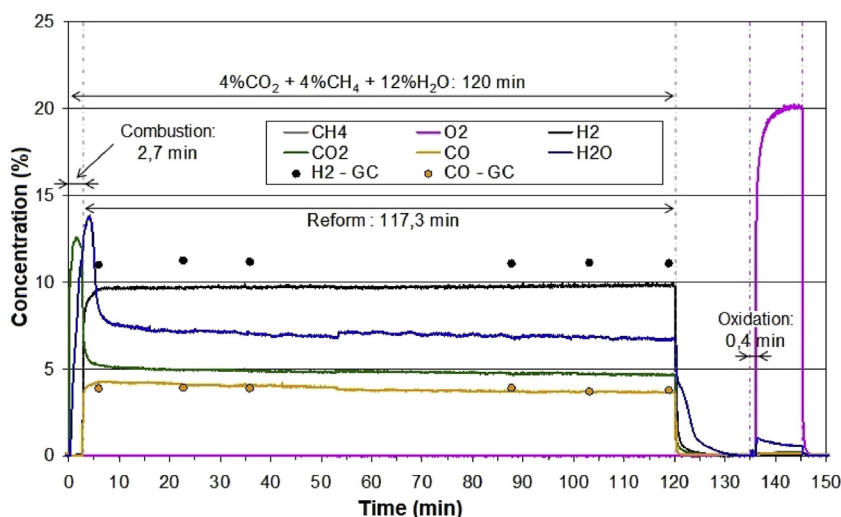


Fig. 12 – SRB with Ru catalyst (CH₄:CO₂ = 1:1; steam/biogas 1.5; pressure 1 bar; GHSV = 780 h⁻¹).

Table 3 – Comparison of Nickel and Ruthenium catalysts from the performance evaluation.

	7.4% Ni/NiAl ₂ O ₄ /γ-Al ₂ O ₃	3.1% Ru/γ-Al ₂ O ₃
Reduction temperature	800 °C	470 °C
Temperature for efficient reforming reactions	850 °C	700 °C
Carbon deposition or catalyst deactivation	None	None
H ₂ /CO ratio for biogas composition (CH ₄ :CO ₂ = 1.5:1/CH ₄ :CO ₂ = 1:1)	2.9/2.4	3/2.4
H ₂ yield	60%	60%

and H₂ are produced (characteristic of dry reforming) from 470 °C, i.e. a temperature that is much lower than that obtained with the Ni catalyst (800 °C).

The Ni catalyst proved efficient in reforming reactions whose temperature is equal to or greater than 850 °C. At lower temperatures, the catalyst was not enough for activating the reforming reaction. As the amount of CO₂ increased in the biogas composition (CH₄:CO₂ = 1.5:1 to CH₄:CO₂ = 1:1), there was a decrease in H₂/CO ratio from 2.9 to 2.4 by an increase in the dry reforming rate when the nickel catalyst was used. During the experiments, no carbon deposition or catalyst deactivation was noted.

On the other hand, the reactions with the Ru catalyst presented an H₂/CO ratio which is closer to the value found in literature for the steam reforming (H₂/CO = 3), thus indicating that this material is efficient and selective for this reaction. In addition, the working temperature is much lower than the one used with the Ni catalyst. There was no deactivation, nor a significant formation of carbon deposition in any of the experiments, which suggests great durability of these catalysts without the need for frequent regenerations.

When comparing the performance of the Ni catalyst in Fig. 9 working at 850 °C to the Ru catalyst shown in Fig. 11 at 700 °C, H₂ yield was very similar (~60%) and H₂/CO ratio was 2.9 and 3, respectively, thus showing that both catalysts have a similar behavior when they are used in the steam reforming of biogas. The same conclusion is reached when comparing the performance of catalysts in the long-term stability test by using a ratio of CH₄:CO₂ = 1:1. From Figs. 10 and 12, it can be observed that the concentrations of gases it produced are almost the same as the H₂ yield of 47.5% and a H₂/CO ratio of 2.4. The main difference between both catalysts was in the yield of CO₂ production, being of 19.5% for Ni catalyst and 25% for Ru catalyst.

It is known that the use of noble metals such as Rh, Pd, Ir, Pt and Ru lead to an improvement in catalyst activity, thus making it more stable and attenuating coke formation [47] in comparison with the Ni catalyst which has the limitation of coke deposition and deactivation susceptibility at higher temperatures [17,22]. However, a nickel catalyst with an interfacial nickel aluminate layer (NiAl₂O₄) allows a prominent performance with high activity [30,36]. On the other hand, the use of noble metals in catalysts is limited to experimental tests in laboratory, not being developed commercially for economic reasons [3]. Therefore, by considering the results achieved in this study, the 7.4% Ni/NiAl₂O₄/γ-Al₂O₃ catalyst is proved suitable for the steam reforming of biogas, which it is less expensive than the Ru catalyst with almost the same performance. Furthermore, this type of catalyst has a great potential for industrial application in the future [27].

Conclusion

Steam reforming of biogas has been studied with two types of catalysts: nickel 7.4% Ni/NiAl₂O₄/γ-Al₂O₃ and Ruthenium 3.1% Ru/γ-Al₂O₃. The following conclusions can be drawn:

- 1) The Ni catalyst proved efficient in reforming reactions whose temperature is equal to or higher than 850 °C. At lower temperatures, the catalyst was not enough for the steam reforming reaction activation.
- 2) Both catalysts showed the same behavior with an increase in CO₂ concentration in the gas feed, which leads to decrease in H₂/CO ratio and H₂ yield, thus showing that optimal performance is achieved at a CH₄:CO₂ ratio of 1.5:1.
- 3) Further investigation on carbon deposition was conducted by characterizing the catalysts used in the steam reforming of biogas. Both catalysts showed no deactivation during these tests and the amount of carbon formed was at very low levels, and there was no production of CO or CO₂, which could be found by mass spectrometry, thus indicating that these materials are efficient and selective for the steam reforming of biogas with high resistance to coke formation.
- 4) An excellent reactivity of 7.4% Ni/NiAl₂O₄/γ-Al₂O₃ catalyst is a result of the existence of an interfacial NiAl₂O₄ layer that stabilizes the formation of low size nickel particles, and the high dispersion and distribution of the active phase on the support effectively suppress catalyst sintering, thus leading to practically the same performance as the Ru catalyst.

Acknowledgements

This work was financed by FAPESP (São Paulo State Research Foundation, process number 06/52260-2). The authors are also grateful to the Coordination for the Improvement of Higher Education Personnel (CAPES), from the Brazilian Ministry of Education (MEC). The authors would also like to acknowledge the language revision services provided by FAV Language Services.

REFERENCES

- [1] Bollini L, Silveira JL, Evaristo M, Tuna CE, Machin EB, Pedrosa DT. Hydrogen production by biogas steam reforming: a technical, economic and ecological analysis. *Renew Sustain Energy Rev* 2013;28:166–73.

- [2] Xu J, Zhou W, Li Z, Wang J, Ma J. Biogas reforming for hydrogen production over a Ni–Co bimetallic catalyst: effect of operating conditions. *Int J Hydrogen Energy* 2010;35:13013–20.
- [3] Therdthianwong S, Siangchin C, Therdthianwong A. Improvement of coke resistance of Ni/Al₂O₃ catalyst in CH₄/CO₂ reforming by ZrO₂ addition. *Fuel Process Technol* 2007;9:0–8.
- [4] Rick R, Pires E, Jose H, Sato M, Coimbra-arau CH. Overview of hydrogen production technologies from biogas and the applications in fuel cells. *Int J Hydrogen Energy* 2013;38:5215–25.
- [5] ENERGY USD-EEAR. Hydrogen, fuel cells & infrastructure technologies program. 2005. <http://www1.eere.energy.gov/hydrogenandfuelcells/mypp/>.
- [6] Steinberg M. The Hy-C process (thermal decomposition of natural gas) potentially the lowest cost source of hydrogen with the least CO₂ emission. *Energy Convers Manag* 1995;36:791–6.
- [7] Poirier MG, Sapundzhiev C. Catalytic decomposition of natural gas to hydrogen for fuel cell applications. *Int J Hydrogen Energy* 1997;22:429–33.
- [8] Effendi A, Hellgardt K, Zhang Z, Yoshida T. Optimising H₂ production from model biogas via combined steam reforming and CO shift reactions. *Fuel* 2005;84:869–74.
- [9] Formanski V, Kalk T, Roes J. Compact hydrogen production systems for solid polymer fuel cells. *J Power Sources* 1998;71:199–207.
- [10] Villacampa JI, Royo C, Romeo E, Montoya JA, Del Angel P, Monzón A. Catalytic decomposition of methane over Ni–Al₂O₃ coprecipitated catalysts: reaction and regeneration studies. *Appl Catal A Gen* 2003;252:363–83.
- [11] Benito M, Garc S, Garc L, Daza L. Development of biogas reforming Ni–La–Al catalysts for fuel cells. *J Power Sources* 2007;169:177–83.
- [12] Kolbitsch P, Pfeifer C, Hofbauer H. Catalytic steam reforming of model biogas. *Fuel* 2008;87:701–6.
- [13] Barrai F, Jackson T, Whitmore N, Castaldi MJ. The role of carbon deposition on precious metal catalyst activity during dry reforming of biogas. *Catal Today* 2007;129:391–6.
- [14] Shuyan W, Lijie Y, Huilin L, Yurong H. Simulation of effect of catalytic particle clustering on methane steam reforming in a circulating fluidized bed reformer. *Chem Eng J* 2008;139:136–46.
- [15] Ma Y, Xu Y, Demura M, Hirano T. Catalytic stability of Ni₃Al powder for methane steam reforming. *Appl Catal B Environ* 2008;80:15–23.
- [16] Sun H, Wang H, Zhang J. Preparation and characterization of nickel – titanium composite xerogel catalyst for CO₂ reforming of CH₄. *Appl Catal B Environ* 2007;73:158–65.
- [17] Goula MA, Charisiou ND, Papageridis KN, Delimitis A, Pachatouridou E, Iliopoulou EF. Nickel on alumina catalysts for the production of hydrogen rich mixtures via the biogas dry reforming reaction: influence of the synthesis method. *Int J Hydrogen Energy* 2015;40:9183–200.
- [18] Urasaki K, Sekine Y, Kawabe S, Kikuchi E, Matsukata M. Catalytic activities and coking resistance of Ni/perovskites in steam reforming of methane. *Appl Catal A Gen* 2005;286:23–9.
- [19] Fonseca A, Assaf EM. Production of the hydrogen by methane steam reforming over nickel catalysts prepared from hydrotalcite precursors. *J Power Sources* 2005;142:154–9.
- [20] Sabirova ZA, Danilova MM, Zaikovskii VI, Kuzin NA, Kirillov VA, Kriger TA, et al. Nickel catalysts based on porous nickel. *Kinet Catal* 2010;49:428–34.
- [21] Taylor K, Mason D, Lo DG. A light hydrocarbon fuel processor producing high-purity hydrogen. *J Power Sources* 2003;117:84–91.
- [22] Xu J, Zhou W, Li Z, Wang J, Ma J. Biogas reforming for hydrogen production over nickel and cobalt bimetallic catalysts. *Int J Hydrogen Energy* 2009;34:6646–54.
- [23] Angeli SD, Pilitsis FG, Lemonidou AA. Methane steam reforming at low temperature: effect of light alkanes' presence on coke formation. *Catal Today* 2015;242:119–28.
- [24] Luna AEC, Iriarte ME. General Carbon dioxide reforming of methane over a metal modified Ni–Al₂O₃ catalyst. *Appl Catal A Gen* 2008;343:10–5.
- [25] Zhang ZL, Tspouriari VA, Efstathiou AM, Verykios XE. Reforming of methane with carbon dioxide to synthesis gas over supported rhodium catalysts: I. Effects of support and metal crystallite size on reaction activity and deactivation characteristics. *J Catal* 1996;158:51–63.
- [26] Therdthianwong S, Summaprasit N. Synthesis gas production from CH₄ reforming with CO₂ over Pd/Al₂O₃ promoted with CeO₂. *Asian J Energy Environ* 2002;3:1–25.
- [27] Avraam DG, Halkides TI, Liguras DK, Bereketidou OA, Goula MA. An experimental and theoretical approach for the biogas steam reforming reaction. *Int J Hydrogen Energy* 2010;5:1–10.
- [28] Zhang ZG, Xu G, Chen X, Honda K, Yoshida T. Process development of hydrogenous gas production for PEFC from biogas. *Fuel Process Technol* 2004;85:1213–29.
- [29] Lucrédio AF, Assaf JM, Assaf EM. Reforming of a model biogas on Ni and Rh–Ni catalysts: effect of adding La. *Fuel Process Technol* 2012;102:124–31.
- [30] Salhi N, Boulahouache A, Petit C, Kiennemann A, Rabia C. Steam reforming of methane to syngas over NiAl₂O₄ spinel catalysts. *Int J Hydrogen Energy* 2010;6:3–9.
- [31] El Doukkali M, Iriondo A, Arias PL, Requies J, Gandarías I, Jalowiecki-Duhamel L, et al. A comparison of sol-gel and impregnated Pt or/and Ni based γ -alumina catalysts for bioglycerol aqueous phase reforming. *Appl Catal B Environ* 2012;125:516–29.
- [32] Al-Ubaid A, Wolf EE. Steam reforming of methane on reduced non-stoichiometric nickel aluminate catalysts. *Appl Catal* 1988;40:73–85.
- [33] Lif J, Skoglundh M, Löwendahl L. Sintering of nickel particles supported on γ -alumina in ammonia. *Appl Catal A Gen* 2002;228:145–54.
- [34] Zielinski J. Morphology of nickel/alumina. *J Catal* 1982;76:157–63.
- [35] Zhang LF, Lin JF, Yi C. Characterization of dispersion and surface states of NiO/g-alumina and NiO/La₂O₃-g-alumina catalysts. *J Chem Soc Faraday Trans* 1992;88(3):497–502.
- [36] Zhou L, Guo Y, Zhang Q, Yagi M, Hatakeyama J, Li H, et al. A novel catalyst with plate-type anodic alumina supports Ni/NiAl₂O₄/g-Al₂O₃/alloy, for steam reforming of methane. *Appl Catal A Gen* 2008;347:200–7.
- [37] Betancourt P, Rives A, Hubaut R, Scott CE, Goldwasser J. A study of the ruthenium-alumina system. *Appl Catal A Gen* 1998:170.
- [38] Koopman PGJ, Kieboom APG, Van Bekkum H. Characterization of ruthenium catalysts as studied by temperature programmed reduction. *J Catal* 1981;69:172–9.
- [39] Mazzieri V, Coloma-Pascual F, Arcoya A, L'Argentière PC, Fígoli NS. XPS, FTIR and TPR characterization of Ru/Al₂O₃ catalysts. *Appl Surf Sci* 2003;210:222–30.
- [40] Safariamin M, Tidahy LH, Abi-Aad E, Siffert S, Aboukaïs A. Dry reforming of methane in the presence of ruthenium-based catalysts. *Comptes Rendus Chim* 2009;12:748–53.
- [41] Gil A, Diaz A, Gandia LM, Mantes M. Influence of the preparation method and the nature of the support on the stability of nickel catalysts. *Appl Catal A Gen* 1994;109:167–79.

- [42] Thi Q, Bui P, Kim Y, Pil S, Han J, Chul H, et al. Steam reforming of simulated biogas over plate Ni Cr catalysts: influence of pre-oxidation on catalytic activity. *Appl Catal B Environ* 2015;167:335–44.
- [43] Khoshtinat Nikoo M, Amin NAS. Thermodynamic analysis of carbon dioxide reforming of methane in view of solid carbon formation. *Fuel Process Technol* 2011;92:678–91.
- [44] Jiménez-González C, Boukha Z, de Rivas B, Delgado JJ, Cauqui MA, González-Velasco JR, et al. Structural characterisation of Ni/alumina reforming catalysts activated at high temperatures. *Appl Catal A Gen* 2013;466:9–20.
- [45] Boukha Z, Jiménez-González C, de Rivas B, González-Velasco JR, Gutiérrez-Ortiz JI, López-Fonseca R. Synthesis, characterisation and performance evaluation of spinel-derived Ni/Al₂O catalysts for various methane reforming reactions. *Appl Catal B Environ* 2014;158–159:190–201.
- [46] Chang AC, Lee K. Biogas reforming by the honeycomb reactor for hydrogen production. *Int J Hydrogen Energy* 2015:1–8.
- [47] Roy PS, Park CS, Raju ASK, Kim K. Steam-biogas reforming over a metal-foam-coated (Pd-Rh)/(CeZrO₂-Al₂O₃) catalyst compared with pellet type alumina-supported Ru and Ni catalysts. *J CO₂ Util* 2015;12:12–20.
- [48] Ahmed S, Lee SHD, Ferrandon MS. Catalytic steam reforming of biogas—Effects of feed composition and operating conditions. *Int J Hydrogen Energy* 2015;40:105–15.